Effect of cascaded Brillouin lasing due to resonant pumps in a superluminal fiber ring laser gyroscope

M.F. Fouda,[a*] M. Zhou, [b] H.N. Yum,[c] M.S. Shahriar[a,b]

[a]Department of Electrical Engineering and Computer Science, Northwestern University, Evanston, IL 60208

[b]Department of Physics and Astronomy, Northwestern University, Evanston, IL 60208

[c]X-Wave Innovations, Inc, Gaithersburg, MD 20878

Abstract: Fiber ring laser gyroscopes (FRLGs) are among the most sensitive rotation sensors. Recently, we have proposed a scheme for improving the sensitivity of such gyroscopes significantly by using the fast light effect. The resulting device, called the active fast light fiber optic sensor (AFLIFOS), makes use of a pair of counter-propagating superluminal Brillouin lasers in a fiber cavity. Compared to a conventional FRLG, the sensitivity of the AFLIFOS is expected to be enhanced by nearly four orders of magnitude. For both conventional FRLG and the AFLIFOS, the overall sensitivity increases with increasing output power. However, when the power of the pump laser used for producing the Brillouin gain exceeds a threshold value, cascaded higher order Brillouin lasing may occur, thus complicating the dynamics of the AFLIFOS, and limiting the maximum achievable sensitivity. In this work, we experimentally study the parameters that determine the onset of second and third order Brillouin lasing in a fiber cavity. We also analyze how the pump power affects the AFLIFOS operation, and show how the measured threshold for second order Brillouin lasing sets a practical limit for the AFLIFOS sensitivity.

Keywords: Fiber Sensors, Fast Light, Brillouin Laser, superluminal laser

*****Mohamed Fouda**,** E-mail: mfouda@u.northwestern.edu

1. Introduction

A ring laser gyroscope (RLG) is a highly sensitive rotation sensor and is used widely for inertial navigation. In recent years, efforts have been underway to improve the sensitivity of an RLG significantly by making use of the fast light effect [1-5]. Of particular interest in this regard is a fiber ring laser gyroscope (FRLG) based on stimulated Brillouin gain [6]. Several proposals have been put forward for increasing the sensitivity of such an FRLG using the superluminal mode of operation [4, 7-9]. In Ref. 8, we proposed the use of auxiliary fiber resonators coupled to the main fiber resonator to create the superluminal effect. This device is called the active fast light fiber optic sensor (AFLIFOS), which can measure rotation as well as strain. For the AFLIFOS, both the pump and the Brillouin laser, in each direction, are resonant in the fiber cavity. It was shown that about four orders of magnitude enhancement in sensitivity can be achieved for a Brillouin laser power of 1mW. Since the minimum measurable rotation rate is inversely proportional to the square root of the laser power, using higher laser power would improve the gyroscope sensitivity further. However, higher laser power would result in the generation of cascaded higher order Brillouin lasers which would disrupt the superluminal enhancement process. Although the generation of multiple higher order Brillouin laser modes generally require highly nonlinear fibers [10], Erbium-doped fiber [11] or special optical feedback [12], we have observed higher order Brillouin modes in regular single mode fiber loops with resonant pumps. In this paper, we investigate the optical pump power threshold for cascaded Brillouin lasers and how it would limit the ultimate achievable sensitivity of the AFLIFOS.

2. Brillouin gain parameters

We consider first the gain experienced by a Stokes probe coupled to a pump field through the stimulated Brillouin Scattering (SBS) process. The Stokes field propagates in the opposite direction to that of the pump. We assume that the pump is strong enough so that any depletion thereof is negligible. Under this assumption, the slowly varying amplitude of the Stokes field in steady state after the interaction with the pump field can be expressed as $E_S = E_{S0} e^{(\alpha_{Br} + i\beta_{Br})L}$ where E_s is the amplitude after the Brillouin interaction, E_{s0} is the input field amplitude, $\alpha_{Br} = n_0 k \chi'' / 2$ and $\beta_{Br} = n_0 k \chi' / 2$, with

$$\chi' = g_0 I_P (\omega - \omega_L + \omega_B) \Gamma_B \Big/ \left[\rho I + \Gamma_B{}^2 + 4(\omega - \omega_L + \omega_B)^2 \right], \qquad \textbf{(1.a)}$$

$$\chi'' = (g_0 I_P) \Gamma_B{}^2 \Big/ 2 \left[\rho I + \Gamma_B{}^2 + 4(\omega - \omega_L + \omega_B)^2 \right]. \qquad \textbf{(1.b)}$$

Here, n_0 is the fiber refractive index, k is the probe wavenumber, g_0 is the gain coefficient, ω_B is the Brillouin frequency shift, Γ_B is the unsaturated gain linewidth, I_p (I) is the pump (probe) intensity and ω_L (ω) is the pump (probe) frequency. The gain saturation is determined by the parameter ρ such that $\sqrt{\rho I}$ represents the contribution to the gain linewidth due to power broadening. For later reference, we define $G = (g_0 I_P) \Gamma_B{}^2 \Big/ 2 \left[\rho I + \Gamma_B{}^2 \right]$ as the peak value of the Brillouin gain.

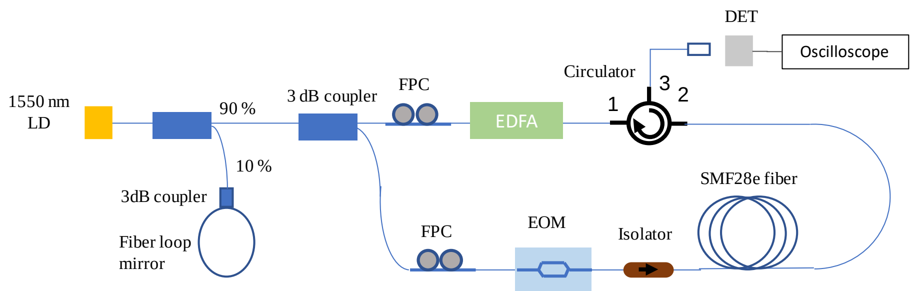

Fig. 1. Experimental setup to measure Brillouin gain spectrum. FPC: fiber polarization controller; EDFA: Er-doped fiber amplifier; EOM: Electro-optic modulator.

Figure 1 shows the experimental setup we used to characterize the Brillouin gain spectrum. The pump light source is a 1550 nm laser diode (LD), with a linewidth of less than 1MHz. The LD output is split into two parts using a 90:10 coupler. At the 10% output port, a 3dB coupler is used to build a fiber loop mirror [13] to reduce the linewidth of the LD via optical feedback. The 90% output is split again by another 3dB coupler. One of the coupler outputs is amplified by an Er-doped fiber amplifier (EDFA) to serve as the Brillouin pump. The other output is modulated by an electro-optic modulator (EOM) to produce the counterpropagating probe. The DC bias of the EOM is adjusted to suppress the fundamental component of the modulated signal. The lower sideband acts as the Brillouin probe. An isolator is used to prevent the amplified pump beam from going back to the laser. The probe interacts with the pump along an 88 m long single mode fiber (Corning SMF-28). Afterwards, the probe is diverted by a circulator to a detector for analysis. The probe frequency ω is scanned around $\omega_L - \omega_B$ to measure the Brillouin gain profile. A scan range of 40MHz with a step size of 0.5MHz was used. Fig. 2(a) shows the observed Brillouin spectrum. The pump power is increased until the gain begins to get saturated. Expressed in Hz, the Brillouin shift frequency $(\omega_B / 2\pi)$ and the unsaturated gain linewidth $(\Gamma_B / 2\pi)$ were measured to be 10.867 GHz and ~10MHz, respectively. The measured value of $(\omega_B / 2\pi)$ is 50 MHz higher than the value found by a previous measurement for SMF-28e reported in Ref. [14]. In addition, the measured linewidth $(\Gamma_B / 2\pi)$ was a factor of 3 less than what was found in that work. It should be noted that a longer fiber (6.4km) and a lower power pump were used in that experiment [14]. Hence, the

Brillouin interaction length was longer and pump depletion [13, 15] occurred to broaden the linewidth by about a factor of three more than in our case. Fig. 2(b) shows how the peak gain value G depends on the pump power. Assuming absence of saturation, the values of G at high pump powers are extrapolated linearly using experimental data at pump powers of 600 and 800mW (square markers). Comparing this extrapolation to the experimental data (triangle markers), we can estimate that the gain starts to saturate at a pump power of ~1.5 W.

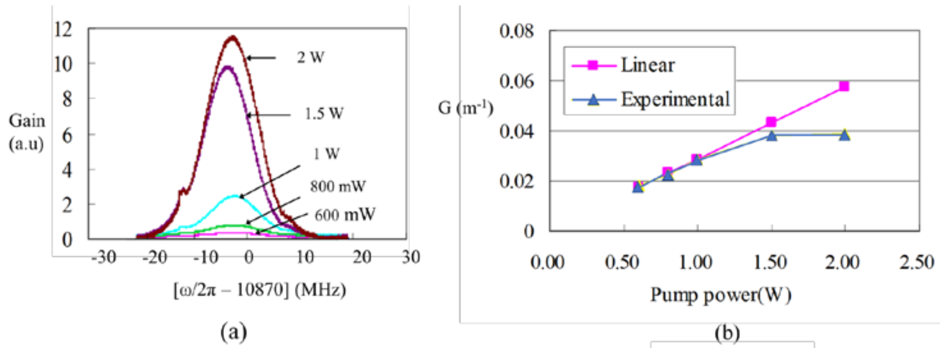

Fig. 2. (a) Brillouin gain spectrum of an 88m SMF-28 single mode fiber plotted versus the probe frequency (b) Gain peak for different values of pump power

3. Brillouin Laser and Higher Order Modes

Next, we study the system used by the active fast light fiber optic sensor (AFLIFOS) presented in ref. 8. In this system, two counterpropagating Brillouin lasers are generated inside a fiber ring cavity. A change in the length of the cavity, induced due to rotation or strain, for example, produces changes in the frequencies of the Brillouin lasers. Two auxiliary cavities, one for each direction, are used to induce negative dispersion. When this dispersion is properly tuned, the changes in the Brillouin laser frequencies are amplified significantly. Hence, the sensitivity of the sensor is correspondingly improved, as discussed in detail later. Here, we investigate the behavior of the Brillouin laser only in the main cavity, and only in one direction, since our goal is to determine the threshold for higher order Brillouin lasing. To ensure single mode operation of the Brillouin laser, the cavity free spectral range (FSR) needs to be larger than the unsaturated Brillouin gain linewidth Γ_B (assuming operation under conditions where the power-broadening does not contribute significantly to the overall gain linewidth). In addition, to ensure that the pump is also resonant in the cavity, the FSR should be a submultiple of the Brillouin frequency shift, i.e., $FSR = \omega_B / (2\pi N)$ where N is an integer. Based on the measured values of ω_B and Γ_B, the fiber cavity was designed to have an FSR = 17.3262 MHz. The experimental setup used to generate the Brillouin laser modes in the resonant cavity is shown in Fig. 3. A fiber loop mirror is used at the 10% output of the first fiber splitter to reduce the linewidth of the laser diode (LD) via optical feedback. The 90% output is passed through an isolator and another fiber splitter. The 10% output of the second splitter is diverted to a Fabry-Perot (FP) cavity, with an FSR of 37 GHz. The 90% splitter output is amplified by an Erbium-doped fiber amplifier (EDFA) to serve as the pump laser. After passing through the circulator, the pump is coupled to the fiber resonator through a variable coupler. The coupling ratio determines the shape of the resonance dip observed in the output of the transmitted pump. At the critical coupling condition [16], the full width at half maximum (FWHM) of the resonance dip is about 0.23MHz. A Piezo-electric transducer (PZT) is used to control the fiber cavity length. Using a lock-in amplifier (LIA) and a servo, the cavity length is locked to the pump resonance. When the circulating pump power inside the fiber cavity exceeds the Brillouin lasing threshold, a counterpropagating Brillouin laser is generated. After being diverted by the circulator, the output of the Brillouin laser is combined with a sample of the pump beam using a beam splitter. The combined beam is then sent to the FP cavity. In order to~~To~~ improve the stability of the system, the fiber cavity is enclosed in a foam box to reduce the air flow affecting the loop and ~~hence~~ any temperature variation. In addition, a battery is used to provide the current for the laser diode, thus~~'s~~ ~~electric driving current is supplied through a battery to reduce~~ strongly suppressing ~~electric~~ current noise. Finally, t~~T~~he laser diode is temperature controlled, in order to improve the frequency stability of the Brillouin pump.

Formatted: Font color: Auto

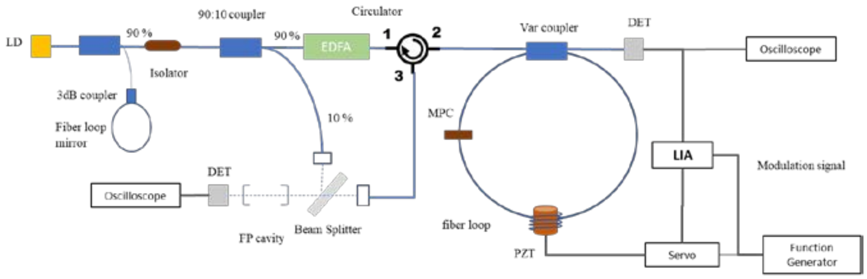

Fig. 3. Schematic of experimental setup for cascaded Brillouin lasers. See text for details.

With the fiber cavity length locked to the pump resonance, the pump power was increased gradually. At low pump powers, with the pump sample blocked, the FP signal shows small peaks at the same positions as the peaks generated when the pump sample is in use. These peaks are due to small reflections of the pump from the variable coupler. When the pump power was increased to around 20 mW, additional peaks, which are shifted from the pump peaks, were observed. Fig. 4(a) shows the FP output in this case. Analysis of the shift of the new peaks from the pump peaks revealed a frequency shift equal to ω_B , confirming that the generated laser is the first order Brillouin mode. Increasing the pump power further led to an increase of the Brillouin laser power. At approximately 60 mW pump power, the second order Brillouin mode was observed, as shown in Fig 4.b. This mode was produced in the same direction as the pump. As such, only a small part of it is reflected by the variable coupler and transferred to the FP cavity. The third order Brillouin mode was observed at 100 mW pump power, as shown in Fig. 4.c.

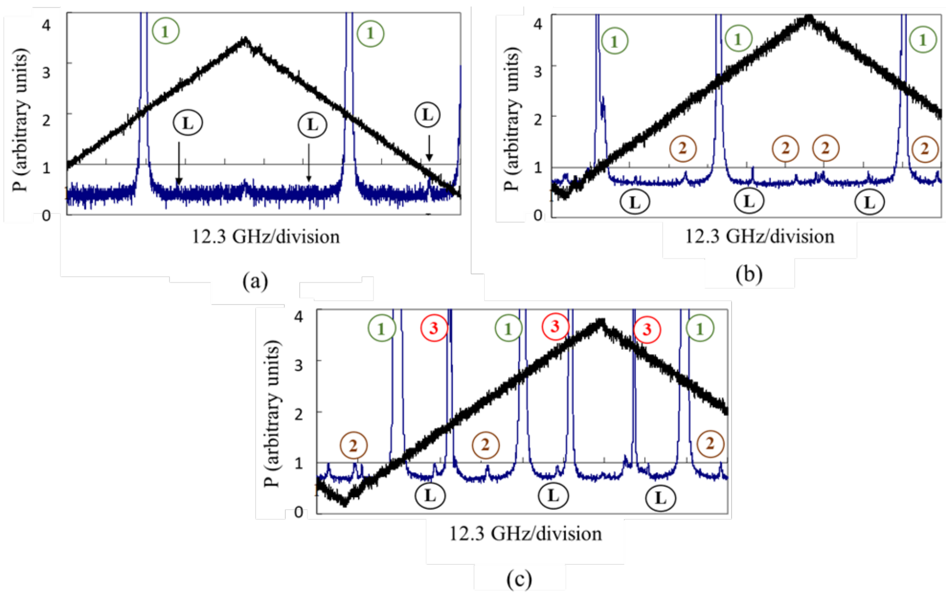

Fig. 4. Fabry-Perot output signal. (a) 1st order Brillouin laser (Pump power: P=20mW), (b) 1st and 2nd order modes (P= 60mW), (c) 1st, 2nd and 3rd order modes (P=100mW). The letter L represents the FP peaks for the pump. Numbers 1-3 represent the FP peaks for the first, second and third order Brillouin modes, respectively.

4. Effect of Brillouin laser power on the performance of the AFLIFOS

In this section, we discuss how increasing the Brillouin laser power and the generation of higher order modes affect the operation of the AFLIFOS. The complete design of the AFLIFOS was presented in ref. 8. For simplicity, we show in Fig. 5.a the basic concept underlying the AFLIFOS.

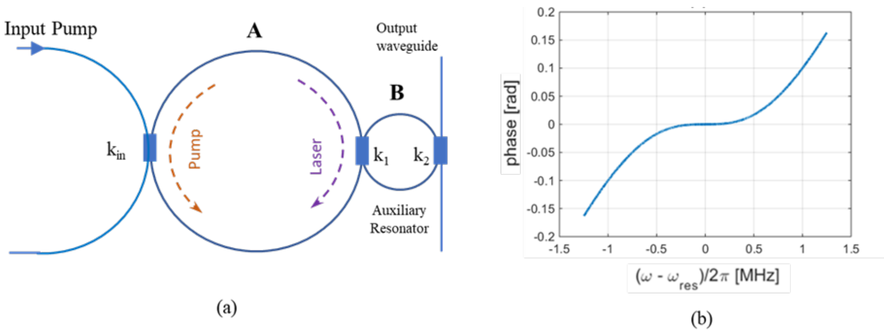

Fig. 5. a) Diagram of the core part of the AFLIFOS b) Brillouin laser roundtrip phase under the superluminal condition. Here ω_{res} is the resonance frequency of both resonators.

Briefly, the pump coupled into the main resonator, A, produces Brillouin lasing. The presence of the auxiliary resonator, B, (with its resonance frequency being at the peak of the Brillouin gain) causes a dip in the gain spectrum for the Brillouin laser, thereby producing anomalous dispersion. It should be noted here that the auxiliary resonator (AR) free spectral range is selected to have a value such that the AR does not have a resonance dip at the pump frequency. Hence, ~~-~~the Brillouin pump ~~undergoes a minimal increased~~experiences negligible loss due to ~~the introduction of~~ the AR. The AFLIFOS superluminal condition is satisfied when the group index of refraction n_g at the laser frequency is close to zero. The sensitivity enhancement of the AFLIFOS is proportional to the reciprocal of n_g [4].

Formatted: Font color: Auto

To achieve a near zero group index of refraction, the phase shift produced by the auxiliary resonator at the laser frequency should compensate other phase variations in the system, as follows:

$$\frac{d\theta}{d\omega}+\frac{d\theta_{Br}}{d\omega}=-\frac{n_0}{c}L. \qquad (2)$$

Here, θ is the phase shift produced by the auxiliary fiber resonator, n_0 is the fiber refractive index, L is the length of the main fiber loop and $\theta_{Br}=\beta_{Br}L$ is the phase accumulated due to the Brillouin gain process. When Eq. (2) is satisfied, the roundtrip phase of the superluminal Brillouin laser has a plateau around the resonance frequency (which is the same for both resonators), as shown in Fig. 5.b. The group index of refraction is proportional to the derivative of the roundtrip phase, resulting in a very small value of n_g and in turn a significant sensitivity enhancement. This requires the parameters of the auxiliary fiber resonator, such as the coupling coefficient to the main fiber loop, k_1, and to the output fiber, k_2, to be carefully selected. As shown in Eq. (2), these parameters depend on θ_{Br}, which in turn depends on the parameters of the Brillouin gain process. In our analysis, we have used the experimental values of Γ_B and ω_B presented earlier, a loop length L = 9.939 m, n_0 = 1.45 and a fiber loss coefficient α = 14 dB/km. Assuming a value of k_1 = 0.05, the superluminal condition can be achieved using an auxiliary resonator length L_{AR} = 1.656 m and k_2 =0.1452.

For an FRLG operating without the superluminal effect, a rotation rate Ω leads to a change of the resonance frequency due to the Sagnac effect, given by:

$$\delta\omega_0 = \frac{\omega_0}{cn_0}\frac{4\Omega A}{L}, \tag{3}$$

where A is the area of the fiber loop. The rotation rate is equivalent to a change of the fiber loop length $\delta L = 2\Omega A / cn_0$. The superluminal operation of the AFLIFOS leads to an enhancement of the resonance frequency by the factor of $\xi = \delta\omega_S / \delta\omega_0$, where $\delta\omega_S$ is the superluminal resonance frequency shift. Since the measurement of rotation requires the measurement of the frequency shift, the minimum detectable rotation rate $\Omega_{\min}$ depends on the quantum-noise limited spectral uncertainty $\Delta\omega_{QN}$. The spectral uncertainty is a function of the Schawlow-Townes linewidth γ_{STL} and the measurement bandwidth $\gamma_m = 1/\tau_m$:

$$\Delta\omega_{QN} = \sqrt{\gamma_{STL}\gamma_m} = \frac{1}{\tau_c}\sqrt{\frac{\hbar\omega_0}{P\tau_m}}, \tag{4}$$

where τ_m is the measurement time, P is the Brillouin laser power, $\tau_c = Q/\omega_0$ is the empty cavity decay time, with Q being the empty cavity quality factor [9]. The minimum detectable rotation rate achievable by the AFLIFOS at a specific Brillouin laser power P is obtained by equating the enhanced frequency shift of the AFLIFOS, $\delta\omega_S$, to the spectral uncertainty $\Delta\omega_{QN}$. The resulting minimum detectable rotation rate is given by

$$\Omega_{MIN} = \frac{S}{\xi}(P\tau_M)^{-1/2}, \qquad S = \frac{cn_0 L}{4\omega A}\frac{1}{\tau_C}(\hbar\omega_0)^{1/2}. \tag{5}$$

For the AFLIFOS parameters considered above, a minimum detectable rotation rate of $\Omega_{MIN} = 2.8\times10^{-12}$ rad/sec can be achieved for a laser power of P = 1 mW and measurement time τ_m

= 1 sec, for an enhancement factor of $\xi \simeq 300$. It is clear from Eq. (5) that Ω_{MIN} decreases (improved sensitivity) as P increases if other parameters are kept the same. The other variable in Eq. (5) is the resonance frequency enhancement ξ. To investigate how ξ depends on the laser power, we recall that $\xi = \delta\omega_S / \delta\omega_0$ where $\delta\omega_S$ is the superluminal resonance frequency shift due to a perturbation δL in the loop length. The superluminal resonance frequency $\omega_S = \omega_0 + \delta\omega_S$ can be calculated from the laser phase condition:

$$\frac{\omega_S}{c_0} n_0(\omega_S)(L+\delta L) + \theta(\omega_S) + \theta_{Br}(\omega_S) = 2\pi m. \quad (6)$$

The phase contribution from the Brillouin gain process θ_{Br} can be calculated from the laser gain condition. At the lasing condition, the Brillouin gain is equal to the loss in the main fiber loop, including the loss due to coupling to the auxiliary cavity:

$$\alpha_{Br} = -\alpha - \frac{1}{L+\delta L}\ln\left(\left|T_{AR}\right|\right). \quad (7)$$

Here, α is the fiber loss coefficient and T_{AR} is the transfer function the auxiliary resonator. From Eq. (1), the Brillouin gain and phase coefficients are related by

$$\beta_{Br} = 2(\omega - \omega_L + \omega_B)\alpha_{Br} / \Gamma_B. \quad (8)$$

Since $\theta_{Br} = \beta_{Br}(L+\delta L)$, Eq. (6) can be written as:

$$\frac{\omega_S}{c_0} n_0(\omega_S)(L+\delta L) + \theta(\omega_S) + 2\frac{(\omega_S - \omega_L + \omega_B)}{\Gamma_B}(-\alpha L - \alpha\delta L - \ln\left(\left|T_{AR}\right|\right)) = 2\pi m. \quad (9)$$

Equation (9) is independent of the pump power and the Brillouin laser power. Hence, the superluminal resonance frequency ω_S and the resonance frequency enhancement ξ are independent on the Brillouin laser power.

Thus, the minimum detectable rotation rate depends only on the laser power as $\Omega_{MIN} \propto P^{-1/2}$. The sensitivity enhancement η can be defined as the factor by which the value of Ω_{MIN} is reduced due to the superluminal effect; as such, $\eta \propto P^{1/2}$. Thus, in general, increasing the pump power would improve the sensitivity. For example, for the AFLIFOS parameters considered earlier, if the Brillouin laser power is increased to P = 10 mW, the minimum detectable rotation rate would be reduced by a factor of $\sqrt{10}$ to $\Omega_{MIN} = 8.8\times10^{-13}$ rad/sec. However, in practice, such an improvement in sensitivity by increasing the Brillouin laser power may not be possible, beyond a certain value, due to the generation of higher order Brillouin modes. As shown earlier in the experimental results, an increase in the pump power beyond some value leads to the generation of the second order Brillouin mode. These modes will cause significant complications in the system due to the existence of multiple beat frequencies. Thus, the pump power at which second order Brillouin mode appears represents the maximum pump power that can be used for the AFLIFOS, hence limiting the degree of enhancement achievable.

Conclusion

We have experimentally investigated the thresholds for higher order Brillouin modes in a resonant fiber cavity. This kind of cavity is the core component of the active fast light fiber optic sensor (AFLIFOS) proposed previously by us. The analysis of the AFLIFOS system indicates that increasing the pump power can lead to improvement in the system sensitivity. However, if the pump power exceeds the threshold value for generating second order Brillouin mode, the presence of the additional frequencies would be inconsistent with the operation of the AFLIFOS. Thus, the maximum sensitivity achievable in an AFLIFOS is limited by the value achieved for a pump power just below the threshold for second order Brillouin lasing.

Acknowledgement

This work has been supported in part by NASA Grant # NNX16CM03C.

Reference

1. A.B. Matsko, A.A. Savchenkov, V.S. Ilchenko, and L. Maleki, *Optical gyroscope with whispering gallery mode optical cavities*, Optics Communications **233**, (2004).
2. D.D. Smith, H.A. Luckay, H. Chang, and K. Myneni, *Quantum-noise-limited sensitivity enhancement of a passive optical cavity by a fast-light medium*, Physical Review A **94**, (2016).
3. T. Qu, K. Yang, X. Han, S. Wu, Y. Huang, and H. Luo, *Design of a superluminal ring laser gyroscope using multilayer optical coatings with huge group delay*, Sci Rep **4**, (2014).
4. M.S. Shahriar, G.S. Pati, R. Tripathi, V. Gopal, M. Messall, and K. Salit, *Ultrahigh enhancement in absolute and relative rotation sensing using fast and slow light*, Physical Review A **75**, (2007).
5. J. Yablon, Z.F. Zhou, M.C. Zhou, Y. Wang, S. Tseng, and M.S. Shahriar, *Theoretical modeling and experimental demonstration of Raman probe induced spectral dip for realizing a superluminal laser*, Optics Express **24**, (2016).
6. F. Zarinetchi, S.P. Smith, and S. Ezekiel, *Stimulated Brillouin fiber-optic laser gyroscope*, Opt Lett **16**, (1991).

7. M.A. Terrel, M.J.F. Digonnet, and S. Fan, *Coupled resonator gyroscopes: what works and what does not*, **7612**, (2010).
8. O. Kotlicki, J. Scheuer, and M.S. Shahriar, *Theoretical study on Brillouin fiber laser sensor based on white light cavity*, Optics Express **20**, (2012).
9. M.Z.Z. Zouh, M. Fouda, N. Condon, J. Scheuer, and S.M. Shahriar, *Fast-light Enhanced Brillouin Laser Based Active Fiber Optic Sensor for Simultaneous Measurement of Rotation and Strain* Journal of Lightwave Technology (2017).
10. B.A. Ahmad, A.W. Al-Alimi, A.F. Abas, M. Mokhtar, S.W. Harun, and M.A. Mahdi, *Compact Brillouin Fiber Laser Based on Highly Nonlinear Fiber With 51 Double Spacing Channels*, Ieee Photonics Journal **4**, (2012).
11. S. Shahi, S.W. Harun, and H. Ahmad, *Multi-wavelength Brillouin fiber laser using a holey fiber and a bismuth-oxide based erbium-doped fiber*, Laser Physics Letters **6**, (2009).
12. S.W. Harun, M.R. Shirazi, and H. Ahmad, *A new configuration of multi-wavelength Brillouin fiber laser*, Laser Physics Letters **5**, (2008).
13. S. Feng, Q. Mao, L. Shang, and J.W.Y. Lit, *Reflectivity characteristics of the fiber loop mirror with a polarization controller*, Optics Communications **277**, (2007).
14. A. Loayssa, R. Hernandez, D. Benito, and S. Galech, *Characterization of stimulated Brillouin scattering spectra by use of optical single-sideband modulation*, Optics Letters **29**, (2004).
15. M. Nikles, L. Thevenaz, and P.A. Robert, *Brillouin gain spectrum characterization in single-mode optical fibers*, Journal of Lightwave Technology **15**, (1997).
16. A. Yariv, *Universal relations for coupling of optical power between microresonators and dielectric waveguides*, Electronics Letters **36**, (2000).